LOW-COMPLEXITY FREQUENCY-DOMAIN GSC FOR BROADBAND BEAMFORMING

Wei Liu, Stephan Weiss, and Lajos Hanzo

Communications Research Group
Dept. of Electronics & Computer Science
University of Southampton, SO17 1BJ, U.K.

ABSTRACT

This paper proposes a new method to reduce the computational complexity of the frequency-domain GSC. In this proposed GSC structure, the column vectors of the blocking matrix constitute a series of bandpass filters, which decompose the impinging signals into components of specific DOA angles and frequencies and lead to band-limited spectra of blocking matrix outputs. When applying a DFT to each of these outputs, some of the frequency bins of the DFT are zero and can be omitted from the adaptive processing. This, together with partial adaptivity of the beamformer, results in a low computational complexity system.

1. INTRODUCTION

Adaptive beamforming has found many applications in various areas ranging from sonar and radar to wireless communications. It is based on a technique where, by adjusting the weights of a sensor array, a prescribed spatial and spectral selectivity is achieved. A broadband beamformer with M sensors receiving a signal of interest from the direction of arrival (DOA) angle θ is shown in Fig. 1, where f_m, $m = 0(1)M-1$, are the attached filters to each sensor. As an alternative beamforming structure for the linearly constrained minimum variance (LCMV) beamformer [1], the generalised sidelobe canceller (GSC) was proposed in [2], which transforms the constrained optimisation problem into an unconstrained one.

As the time-domain GSC using least mean square (LMS) algorithms suffers from a low convergence rate when the condition number of the input correlation matrix increases, a frequency-domain GSC (FGSC) was proposed by Chen and Fang [3]. In their work, a one-dimensional discrete Fourier transform (DFT) is used on each of the tap-delay lines at the output of the blocking matrix. Therefore, an LMS algorithm with self-orthogonalising property is applied. With two-dimensional transform-domain GSC introduced in the reference [4], the convergence rate is improved further due to the removal of both the spatial and temporal correlation. With the advantage of higher convergence speed, the transform-domain GSC however poses the problem of large computational complexity.

In this paper, a new realisation of the FGSC called subband-selective FGSC (SSFGSC) will be proposed to reduce its computational complexity. In our SSFGSC, the blocking matrix of the GSC is constructed such that its columns constitute a series of bandpass filters, which select signals with specific direction of arrival angles and frequencies. This results in bandlimited spectra of the blocking matrix outputs. When applying the DFT to each of these tap-delay lines, the frequency-bins of the DFT outputs corresponding to the stopbands of these spectra will be approximately zero and can be omitted from the following adaptive processing, which reduces the computational complexity greatly. Because of the finite-duration effect of this DFT, we need to apply a window function with narrow bandwidth to the tap-delay line signals before performing the DFT, which is not necessary in the original FGSC.

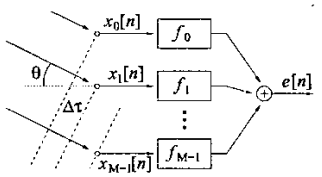

Fig. 1: A broadband beamformer with linear array.

The paper is organised as follows. Sec. 2 briefly reviews the frequency-domain realisation of the GSC structure. The structure and design of our novel subband-selective FGSC is introduced in Sec. 3 and 4, respectively. Simulations underlining the benefit of our proposed method are discussed in Sec. 5 and conclusions drawn in Sec. 6.

2. FREQUENCY-DOMAIN GENERALISED SIDELOBE CANCELLER

A linearly constrained minimum variance (LCMV) beamformer [1] performs the minimization of the variance or power of the beamformer output with respect to some given spatial and spectral constraints. For a broadband beamformer with M sensors and J filter taps following each sensor, the output $e[n]$ can be expressed as

$$e[n] = \mathbf{w}^H \mathbf{x}, \tag{1}$$

where coefficients and input sample values are defined as

$$\mathbf{w} = \left[\mathbf{w}_0^T \ \mathbf{w}_1^T \ \dots \ \mathbf{w}_{J-1}^T\right]^T \tag{2}$$

$$\mathbf{w}_j = [w_{0,j} \ w_{1,j} \ \dots \ w_{M-1,j}]^H \tag{3}$$

$$\mathbf{x} = \left[\mathbf{x}^T[n] \ \mathbf{x}^T[n-1] \ \dots \ \mathbf{x}^T[n-J+1]\right]^T \tag{4}$$

$$\mathbf{x}[n-j] = [x_0[n-j] \ x_1[n-j] \ \dots \ x_{M-1}[n-j]]^T \tag{5}$$

Each vector $\mathbf{w}_j$, $j = 0(1)J-1$, contains the M *complex conjugate* coefficients sitting at the jth tap position of the M attached filters in Fig. 1 and $\mathbf{x}[n-j]$, $j = 0(1)J-1$, holds the jth data slice corresponding to the jth coefficient vector $\mathbf{w}_j$.

The LCMV problem can be formulated as

$$\min_{\mathbf{w}} \mathbf{w}^H \mathbf{R}_{xx} \mathbf{w} \qquad \text{subject to} \qquad \mathbf{C}^H \mathbf{w} = \mathbf{f}\,, \tag{6}$$

where $\mathbf{R}_{xx}$ is the covariance matrix of observed array data in $\mathbf{x}$, $\mathbf{f}$ is the $J \times 1$ response vector and $\mathbf{C}$ is an $MJ \times J$ constraint matrix.

$$\mathbf{C} = \begin{bmatrix} \mathbf{c} & & \mathbf{0} \\ & \ddots & \\ \mathbf{0} & & \mathbf{c} \end{bmatrix} \quad \text{with } \mathbf{c} \in \mathbb{C}^{M\times 1}. \tag{7}$$

The constraint optimisation in (6) can be conveniently solved using a GSC [2], which performs a projection of the data onto an unconstrained subspace by means of a blocking matrix $\mathbf{B}$ and a quiescent vector $\mathbf{w}_q$ shown in the frequency-domain GSC of Fig. 2, where

$$d[n] = \mathbf{w}_q^H \cdot \mathbf{x}_n \qquad \text{with} \quad \mathbf{w}_q = \mathbf{C}(\mathbf{C}^H\mathbf{C})^{-1}\mathbf{f}\quad , \tag{8}$$

and $\mathbf{B} \in \mathbb{C}^{M\times L}$

$$\mathbf{B} = [\mathbf{b}_0\ \mathbf{b}_1\ \ldots\ \mathbf{b}_{L-1}], \tag{9}$$

$$\mathbf{b}_l = [b_l[0]\ b_l[1]\ \ldots\ b_l[M-1]]^H. \tag{10}$$

To receive the desired signal from broadside,the blocking matrix $\mathbf{B}$ must satisfy

$$\mathbf{c}^H\mathbf{B} = \mathbf{0}. \tag{11}$$

The blocking matrix output $\mathbf{u}[n] = [u_0[n]\ u_1[n] \ldots u_{L-1}[n]]$ is obtained by $\mathbf{u}[n] = \mathbf{B}^H\mathbf{x}[n]$, then a J-point DFT is applied to each of the tap-delay vectors $\mathbf{u}_l[n]$, $l = 0(1)L-1$, where

$$\mathbf{u}_l[n] = [u_l[n]\ u_l[n-1]\ \ldots\ u_l[n-J+1]]^T\ . \tag{12}$$

The output of the lth DFT is

$$\mathbf{v}_l[n] = \mathrm{DFT}\{\mathbf{u}_l[n]\}, \tag{13}$$

where $\mathbf{v}_l[n] = [v_{l,0}[n]\ v_{l,1}[n]\ \ldots\ v_{l,J-1}[n]]^T$. Now we write all the DFT outputs into a single vector:

$$\mathbf{v}[n] = \left[\mathbf{v}_0^T\ \mathbf{v}_1^T\ \ldots\ \mathbf{v}_{L-1}^T\right]^T. \tag{14}$$

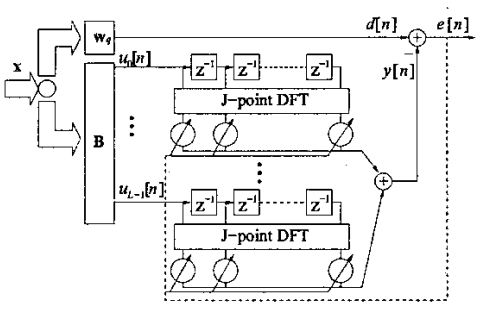

Fig. 2: A general frequency-domain GSC structure.

Therefore $y[n] = \tilde{\mathbf{w}}^H\mathbf{v}[n]$, where $\tilde{\mathbf{w}}$ is the weight vector including all the corresponding weights in the frequency-domain LMS algorithm and updated continually to minimise the power of the error signal $e[n] = d[n] - y[n]$ by a self-orthogonalising LMS algorithm [5] :

$$\tilde{\mathbf{w}}[n+1] = \tilde{\mathbf{w}}[n] + 2\gamma e^*[n]\mathbf{R}_{vv}^{-1}\mathbf{v}[n], \tag{15}$$

where $\mathbf{R}_{vv} = \mathbf{R}_{vv} = \varepsilon\{\mathbf{v}[n]\mathbf{v}^H[n]\}$ and $0 < \gamma < \frac{1}{(LJ)}$. Note that $\mathbf{R}_{vv}$ is unknown and must be estimated.

Although the FGSC accellerates the convergence speed, it also increases the computational complexity of the system. In the next section, instead of using the traditional subtractor structure for the blocking matrix, we sacrifice some degrees of freedom (DOFs) of the system to make a special arrangement for the blocking matrix to reduce the computational complexity of the FGSC.

3. SPATIALLY/SPECTRALLY SUBBAND-SELECTIVE FGSC

Consider a unity amplitude complex input wave with angular frequency ω and DOA angle θ. Referring to Fig. 1, the waveform impinges with a time delay $\Delta\tau$ on adjacent sensors separated by d in a medium with propagation speed c. The received phase vector at the sensor array, $\underline{X}$, is

$$\underline{X} = \left[1\ e^{-j\omega\Delta\tau} \ldots e^{-j\omega(M-1)\Delta\tau}\right]^T \text{with } \Delta\tau = \frac{d}{c}\sin\theta. \tag{16}$$

Assume that the array sensors are spaced by half the wavelength of the maximum signal frequency and the temporal sampling frequency ω_s is twice the maximum signal frequency, i.e. $d = \lambda_s = cT_s$, where T_s is the temporal sampling period. Then, we get $\Delta\tau = T_s\sin\theta$. Noting $\omega T_s = \Omega$, where Ω is the normalised angular frequency of the signal, the phase vector changes to

$$\underline{X} = \left[1\ \ e^{-j\Omega\sin\theta}\ \ \ldots\ \ e^{-j(M-1)\Omega\sin\theta}\right]^T\ . \tag{17}$$

Using the substitution $\Psi = \Omega\sin\theta$, the lth output of the blocking matrix can be denoted as

$$\mathbf{b}_l^H \cdot \underline{X} = \sum_{m=0}^{M-1} b_l[m]\cdot e^{-jm\Psi} = B_l(e^{j\Psi}), \tag{18}$$

with $B_l(e^{j\Psi}) \bullet\!\!-\!\!\circ\, b_l[m]$ being a Fourier transform pair.

When the beamformer is constrained to receive the signal of interest from broadside, the blocking matrix has to suppress any component impinging from $\theta = 0$. Therefore, at $\Psi = 0$ the response of the $\mathbf{b}_l$ has to be zero. Now we arrange these column vectors on the interval $\Psi \in [0;\pi]$ as shown in Fig. 3 [6],

$$B_l(e^{j\Psi}) = \begin{cases} 1 & \text{for } \Psi \in [\Psi_{l,\text{lower}};\ \Psi_{l,\text{upper}}] \\ 0 & \text{otherwise} \end{cases}\ . \tag{19}$$

In reality, the bandpass filters $B_l(e^{j\Psi})$ will not be ideal and hence an overlap and finite transition bands have to be permitted. However, a better design quality can be attained by reducing the number of columns, L, below the limit $M-1$, thus yielding a partially adaptive beamformer by sacrificing some DOFs.

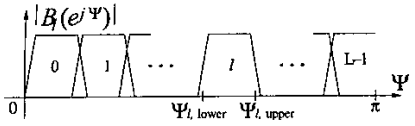

Fig. 3: Arrangement of the L column vectors in $\mathbf{B}$.

From (19), we can get

$$B_l(e^{j\Omega\sin\theta}) = \begin{cases} 1 & \text{for } \Omega \in [\Psi_{l,\text{lower}}; \pi] \\ 0 & \text{otherwise} \end{cases} \quad . \tag{20}$$

By this arrangement, the blocking matrix cannot only decompose the received signals in the spatial, but also in the temporal domain because its column vectors perform a temporal high-pass filtering operation. With increasing l, these filters are associated with a tighter and tighter highpass spectrum and the last output $(L-1)$ only contains the ultimate highpass component. When we apply the frequency-domain LMS algorithm to the output signal $\mathbf{u}_l[n]$, some of the frequency bins will be zero and can be omitted from the following adaptive process. In order to make good use of this property, we need select a good window function to multiply with the time-domain signals prior to applying the DFT.

Now we analysis the computational complexity of this system. For the fully adaptive GSC, $L = M - 1$, so by partial adaptivity, the total weight number is first reduced by $L/(M-1)$. For the FLMS part, if sufficiently selective column vectors $\mathbf{b}_l$ and window function can be designed, under ideal condition, the last DFT output $\mathbf{v}_{L-1}$ will have only two non-zero frequency bins, and $\mathbf{v}_{L-2}$ has four, and so on, while finally only $\mathbf{v}_0$ has no zero frequency bins. Thus, under ideal conditions, the total number of weights to be updated will be reduced further by half. Considering the whole SSFGSC, its computational complexity is listed in Table 1 comparing with the Chen-Fan FGSC (CFGSC).

4. COSINE-MODULATED BLOCKING MATRIX

In our subband-selective FGSC, the blocking matrix plays a central role and the column vector design with a good band-selective property is of great importance.

We may design each of the column vectors independently subject to the constraint (11) [6]. In order to reduce the design and implementation complexity of the blocking matrix, we here use a cosine-modulated version, where all column vectors are derived from a prototype vector by cosine-modulation and the broadside constraint is guaranteed by imposing zeros appropriately on the prototype vector.

Tab. 1: Comparison of computational complexities for SSFGSC and CFGSC:

GSC realisations	complex multiplications per cycle
CFGSC	$(M-1)J\log_2 J + 3.5(M-1)J$
SSFGSC	$LJ\log_2 J + 1.75LJ$

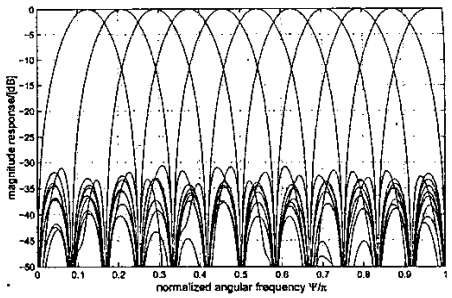

Fig. 4: A design example for a 28×11 blocking matrix.

Assume the prototype vector is $h[m]$, $m = 0(1)M-1$. It is shifted along the frequency axis by $\frac{(2l+3)\pi}{2L+2}$ and $-\frac{(2l+3)\pi}{2L+2}$, respectively and properly added to obtain the lth column vector $b_l[m]$, $l = 0(1)L-1$

$$b_l[m] = h[m]\cos\left[\frac{\pi}{2L+2}(2l+3)(m-\frac{M-1}{2}) - (-1)^l\frac{\pi}{4}\right]. \tag{21}$$

To comply with the broadside constraint $B_l(e^{j\Psi})|_{\Psi=0} = 0$, the frequency response $H(z)$ of $h[m]$ should have one zero at each point of $\omega_l = \pm\frac{(2l+3)\pi}{2L+2}$, $l = 0(1)L-1$. If we factorize $H(z)$ into two parts

$$\begin{aligned} H(z) &= P(z)Q(z), \qquad \text{with} \\ Q(z) &= \prod_{l=0}^{L-1}(1 - e^{j\frac{2l+3}{2L+2}\pi}z^{-1})(1 - e^{-j\frac{2l+3}{2L+2}\pi}z^{-1}), \end{aligned} \tag{22}$$

then the broadside constraint will be automatically satisfied for all the column vectors. Now the free parameters contained in $P(z)$ can be used to optimize its frequency response. By this factorization, the design of the blocking matrix becomes an unconstrained optimization problem of the prototype vector. The objective function we minimize is

$$\Phi = \int_{\Psi_s}^{\pi} \|H(e^{j\Psi})\|^2 d\Psi, \tag{23}$$

where Ψ_s is the stopband cutoff frequency. The optimization problem can be solved conveniently by invoking a nonlinear optimisation software package, such as the subroutines BCONF/DBCONF in the IMSL library [7]. A design example for the blocking matrix with $M = 28$ sensors, and $L = 11$ column vectors is given in Fig. 4.

Note that for $S-1$ order derivative constraints in the blocking matrix [8], we can replace $Q(z)$ by $Q(z)^S$ in (22), but too many DOFs will be sacrificed and a satisfying performance may not be achieved for small-scale arrays.

5. SIMULATIONS AND RESULTS

In our simulation, we use a scenario similar to [3]. A beamformer with $M = 17$ sensors receives the desired signal from broadside with normalised frequency $f = 0.1$ in additive uncorrelated background noise of 20 dB SNR. Three jammers with normalised frequency $0.3, 0.4, 0.25$ come from

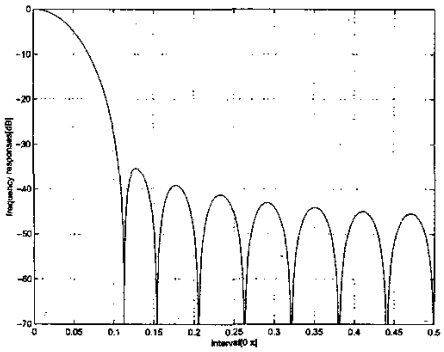

Fig. 5: Frequency response of a 16-tap window function.

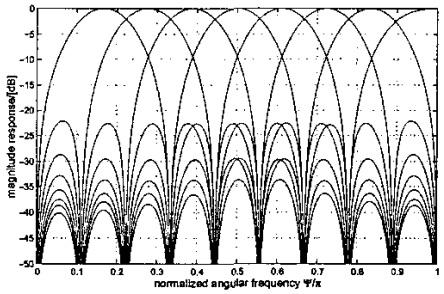

Fig. 6: Frequency responses of 17×8 blocking matrix.

DOA of $\theta = 34°, -49°$ and $-24°$, with jammer-to-signal ratios (JSR) of 20 dB, 40 dB and 30 dB, respectively. A 16-point DFT ($J = 16$) with a window function shown in Fig. 5 is applied in the FLMS algorithm. In our SSFGSC, the dimension of the blocking matrix is 17×8 ($L = 8$) and its frequency responses are shown in Fig. 6. We compare the performance of the SSFGSC with the original time-domain GSC (TDGSC) and the CFGSC. The corresponding step-size parameters γ for the SSFGSC, TDGSC, CFGSC are respectively 1.054×10^{-3}, 1.289×10^{-3} and 1.172×10^{-3} which have been chosen empirically to achieve the same steady-state value of the mean square residual error (MSE).

From the simulation result shown in Fig. 6, we can see that the CFGSC converges much faster than the TDGSC

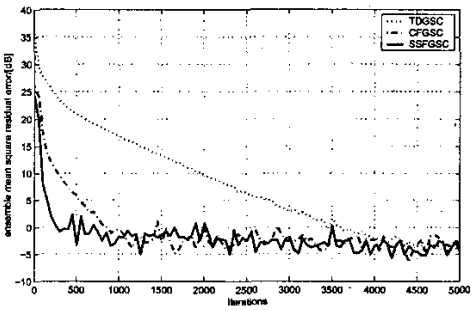

Fig. 7: Learning curves for simulation.

because of the temporal decorrelation effect of the DFT, whereas our new method is faster than the CFGSC due to its combined spatial/temporal decorrelation effect. At last, we need to point out that because of the selected size of the beamfomer and the use of narrowband signal and jammers in our simulation, the sacrifice of some DOFs due to its partial adaptivity did not affect the performance of our SSFGSC. In addition, the proposed SSFGSC only requires about 40% of the complexity needed for the CFGSC.

6. CONCLUSIONS

In this paper, a new realisation of the frequency-domain GSC called subband-selective FGSC has been proposed, where the blocking matrix is constructed such that it decomposes the impinging signals into components of specific DOA angles and frequencies and leads to band-limited spectra of its outputs. When applying a DFT to each of these tap-delay line outputs, some of the frequency bins of the DFT output are zero and can be omitted from the adaptive processing. Together with its partial adaptivity property, this results in a low computational complexity system. Because of its combined spatial/temporal decorrelation effect, it can achieve a faster convergence speed at lower complexity, as shown in our simulation.

7. REFERENCES

[1] O. L. Frost, III, "An Algorithm for Linearly Constrained Adaptive Array Processing," *Proceedings of the IEEE*, vol. 60, no. 8, pp. 926–935, August 1972.

[2] L. J. Griffith and C. W. Jim, "An Alternative Approach to Linearly Constrained Adaptive Beamforming," *IEEE Transactions on Antennas and Propagation*, vol. 30, no. 1, pp. 27–34, January 1982.

[3] Y.H. Chen and H.D. Fang, "Frequency-domain Implementation of Griffiths-Jim Adaptive Beamformer," *J. Acoust. Soc. Am.*, vol. 91, pp. 3354–3366, 1992.

[4] J. An and B. Champagne, "GSC realisations using the two-dimensional transform LMS algorithm," *IEE Proc. Radar, Sonar and Navig.*, vol. Vol.141, pp. pp.270–278, October 1994.

[5] R.D. Gitlin and F.R. Jr. Magee, "Self-orthogonalizing adaptive equalization algorithms," *IEEE Trans. Comm.*, vol. COM-25, pp. 666–672, 1977.

[6] W. Liu, S. Weiss, and L. Hanzo, "A Novel Method for Partially Adaptive Broadband Beamforming," in *Proc. IEEE Workshop on Signal Processing Systems*, Antwerp, Belgium, September 2001.

[7] Visual Numerics Inc., *IMSL Fortran Numerical Libraries.*

[8] K.C. Huarng and C.C. Yeh, "Performance Analysis of Derivative Constraint Adaptive Arrays with Pointing Errors," *IEEE Transactions on Antennas and Propagation*, vol. 40, pp. 975–981, August 1992.